ELECTROMECHANICAL PORTABLE ENERGY HARVESTING DEVICE: ANALYSIS AND EXPERIMENTAL TESTS

Jacek F. Gieras[*], Jae-Hyuk Oh[**], Mihai Huzmezan[**]

[*]University of Technology and Life Sciences
Al. S. Kaliskiego 7, 85-796 Bydgoszcz, Poland, e-mail: jgieras@ieee.org
[**]United Technologies Research Center
411 Silver Lane, East Hartford, CT 06108, USA

Summary: This paper presents the design analysis and performance of an energy harvesting prototype device operating on the principle of electromechanical energy conversion. The input vibration kinetic energy is converted into the output electrical energy. A spring – mass system with moving permanent magnet (PM) is mechanically excited by external vibrations. The voltage is induced in a stationary coil that is embraced by PM poles. When the coil is loaded with an external impedance, an electric current proportional to the induced EMF arises in the external circuit. Fundamental equations for performance calculations have been derived on the basis of elementary beam theory and circuit analysis. A prototype has been built and the calculation results have been validated with the test results.

Keywords: energy harvesting, vibration generator, electromechanical, permanent magnets

1. INTRODUCTION

Self-powered microsystems have recently been considered as a new area of technology development. Interest in self-powered microsystems have been previously addressed in several papers, e.g. [1,6-10]. Main reasons, which stimulate research in this new area are:
- large numbers of distributed sensors,
- sensors located in positions where it is difficult to wire or charge batteries,
- reduction in cost of power and communication,
- Moore's law (the number of transistors per unit area of an IC doubles every 18 months).

Microsystems can be powered by energy harvested from a range of sources present in the environment. Solar cells, thermoelectric generators, kinetic generators, radio power, leakage magnetic or electric fields are just a few examples. In some applications, e.g., container security systems, condition monitoring of machine parts (motors, turbines, pumps, gearboxes), permanent embedding in inaccessible structures (bridges,

roads, towers, masts), or animal tracking, the only source of electrical energy is the kinetic energy.

The harvesting of kinetic energy is the generation of electrical power from the kinetic energy present in the environment. The nature of the kinetic energy harvesting mechanism in a *self contained system* depends upon the nature of the application [6,7,11]. Kinetic energy harvesting devices can be divided into two groups:

- acceleration/vibration and spring mass system devices, e.g. kinetic watches (*Asulub*, *Seiko*), cantilever beam vibration generators, moving magnet linear generators [1,2,3,6,79,12]:
- repeated straining physical deformation devices, e.g. piezoelectric generators or magnetic shape memory generators [8,10,11].

This paper discusses a portable electromechanical energy harvesting device with the magnetic field excitation system integrated with the cantilever beam (i.e. flat spring) and a stationary multiturn coil. The maximum generated energy is when the mechanical resonance occurs, i.e. when the natural frequency of the cantilever beam-based vibrating system is the same or close to the input frequency of vibration. Potential applications include: (1) wireless sensors installed in security systems of containers or trailers, (2) condition-based monitoring of machinery and structures; (3) implanted medical sensors; (4) wearable computers; (5) intelligent environments ("smart space"), etc. The solution designed and presented here is down scalable to the MEMS levels; however, microcollisions, air friction dissipation, and cushioning effects cannot be ignored.

2. FUNDAMENTAL EQUATIONS

A small cantilever beam (spring) with permanent magnets (PMs) fixed to one tip is an integral part of the electromechanical energy harvesting device (Fig. 1). High energy moving PMs induce the EMF in the stationary flat coil. The EMF gives a rise to electric current in an external circuit.

As it is known, the moment of area (inertia) I_a and stiffness k of a cantilever (clamped-free) beam are, respectively,

$$I_a = \frac{1}{12} wt^3 \quad \text{and} \quad k = \frac{3EI_a}{L^3} \tag{1}$$

where w is the width of the cantilever beam (flat spring), $t < w$ is its thickness, L is its length, and E is the Young's modulus (elasticity modulus). Consequently, the natural angular frequency of a cantilever beam for the *n*-th *mode shape* or characteristic deflection shape is expressed as

$$\omega_{nat} = \sqrt{\frac{k}{m}} = \sqrt{\frac{3EI_a}{mL^3}} = a_n \sqrt{\frac{EI_a}{m_b L^3}} \tag{2}$$

Thus, the natural frequency $f_{nat} = \omega_{nat}/(2\pi)$ for the *n*-th mode shape of a cantilever beam can simply be controlled by changing the length L of the beam.
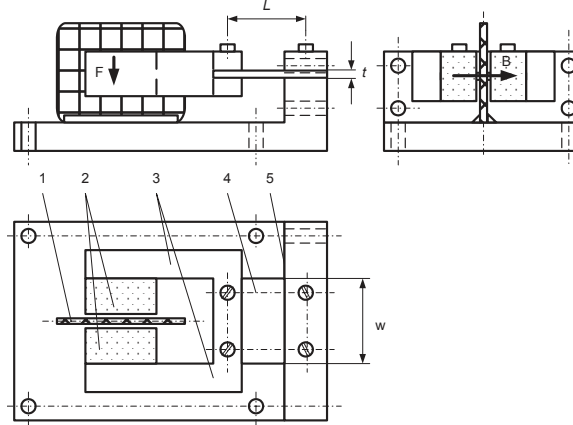
Fig. 1. Principle of operation of the proposed electromechanical energy harvesting device:
1 – stationary coil, 2 – NdFeB PMs, 3 – mild steel magnetic circuit, 4 – cantilever beam
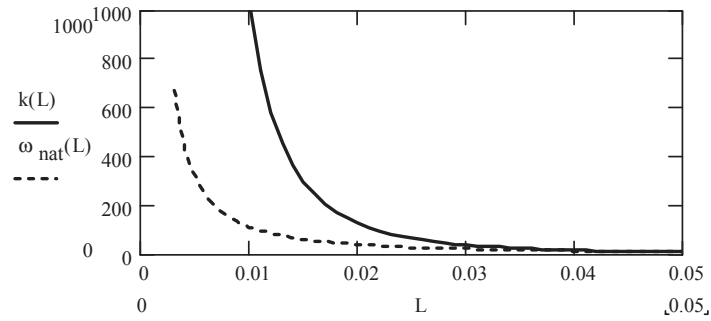(flat spring), 5 – base.

Fig. 2. Spring constant k (N/m) and natural frequency ω_{nat} (1/s) as functions of the length L of
a steel cantilever beam of the tested energy harvesting device ($w = 19.15$ mm, $t = 0.1$ mm,
$E = 210\,000$ N/m)

In elementary beam theory the vibration of a cantilever beam is replaced by a spring-mass system model, as shown in Appendix I. Therefore, the modal mass m in eqn (2) is not equal to the mass m_b of the cantilever beam. For the $n = 1$ mode shape the modal mass is [5]

$$m = 0.2357 m_b \tag{3}$$

and the coefficient $a_n = 3.52$ (see Appendix I).

The operation of an electromechanical energy harvesting device requires a concentrated mass M that is fixed to the tip. This mass represents the mass of PMs and mild steel magnetic circuit. The total modal mass is

$$m = 0.2357 m_b + M \approx M \tag{4}$$

because $m_b << M$. In the investigated prototype the mass of beam $m_b = 0.00015$ kg while the mass of the PM excitation system $M = 0.083$ kg. Thus, for an energy harvesting device the predominant shape mode $n = 1$ and natural angular frequency

$$\omega_{nat} = \sqrt{\frac{3EI_a}{(0.2357m_b + M)L^3}} \approx \frac{1}{2}\sqrt{\frac{Ewt^3}{ML^3}} \qquad (5)$$

The spring constant k and natural frequency ω_{nat} versus the length L of cantilever beam used in the tested energy harvesting device are plotted in Fig. 2.

For a spring – mass system with damper, the cantilever beam with PMs under the effect of *forced motion* will become a single-degree-of-freedom vibrating system that can be described by

$$m\ddot{x}(t) + c\dot{x}(t) + kx(t) = F_m \sin(\omega t) \qquad (6)$$

where $F_m \sin(\omega t)$ is an external force with the amplitude F_m considered for simplicity as changing sinusoidally with the time t and c is the coefficient of a viscous damping. The external force $F_m \sin(\omega t)$ can be produced by a vibrating body on which the cantilever beam with PM is placed. The solution to eqn (6) can be written as

$$x(t) = \sqrt{A^2 + B^2}\,\sin(\omega t + \phi) = X_m \sin(\omega t + \phi) \qquad (7)$$

$$\tan\varphi = \frac{B}{A} \qquad (8)$$

The transfer function and time response are given in Appendix II. By examining eqn (6) it becomes apparent that the energy of vibration is converted into electrical energy with maximum efficiency if the frequency ω the external source of vibration is close to the natural frequency ω_{nat} of the spring-mass system. After solving eqn (6), the forced vibration amplitude X_m (with applied force) and magnification factor MF can be expressed as

$$X_m = \frac{\dfrac{F_m}{k}}{\sqrt{\left[1-\left(\dfrac{\omega}{\omega_{nat}}\right)^2\right]^2 + \left(2\varsigma\dfrac{\omega}{\omega_{nat}}\right)^2}}; \quad MF = \frac{X_m}{\dfrac{F_m}{k}} \qquad (9)$$

where $\varsigma = c/c_c$ is the damping coefficient and $c_c = 2m\omega_{nat}$ is the critical damping coefficient. Both X_m and MF take maximum values for low damping coefficient ζ and frequency of vibration $f_n = \omega_n/(2\pi)$ equal to or very close to $f_{nat} = \omega_{nat}/(2\pi)$. Fig. 3 shows the magnification factor MF according to eqn (13) for three values of damping coefficients $\varsigma = 0.1, 0.2,$ and 0.3.
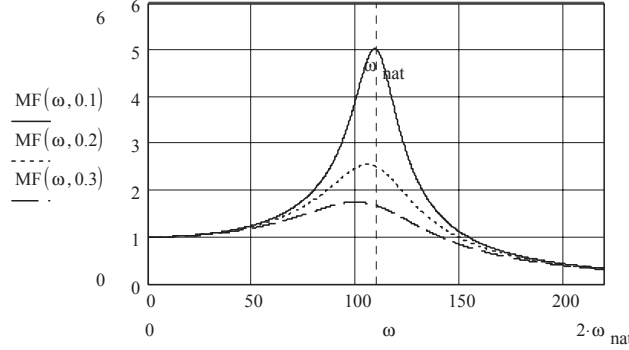
Fig. 3. Damping coefficient *MF* according to eqn (9) as a function of angular frequency ω for three values of damping coefficients ς = 0.1, 0.2, and 0.3.

3. OUTPUT POWER

To generate electrical energy, a stationary coil is placed between the poles of vibrating PMs. The instantaneous voltage induced (or EMF) in a single turn (two conductors) $e(t) = 2\,B\,l_M\,v(x)$ where B is the average magnetic flux density produced by PMs and l_M is the length of the PM (measured along the coil). According to eqn (7), the linear velocity $v(t) = dx(t)/dt = 2\pi\,f\,X_m\cos(\omega t + \phi)$. For N turns the EMF is

$e(t) = 4\pi\,fNBl_M X_m\cos(\omega t + \phi)$. The peak value of the EMF is $E_m = 4\pi\,fNBl_M X_m$ and the *rms* value

$$E = 2\sqrt{2}\pi fNBl_M X_m = 2\sqrt{2}\pi\alpha_i fNB_m l_M X_m \,, \tag{10}$$

where the average-to-peak value ratio of the magnetic flux density can be approximately found as

$$\alpha_i = \frac{B}{B_m} \approx \frac{l_M}{l_M + 2g}\,. \tag{11}$$

Similarly, the electromagnetic reaction force produced by the PM excitation field B and current in the coil I is

$$F_{elm} = \sqrt{2}\alpha_i B_m NIl_M \,. \tag{12}$$

Eqn (12) has been found assuming that the phase angle between the EMF E and current I is zero, i.e. $EI=F_{elm}\,v$. The electromagnetic force F_{elm} is very small because the current in the coil is low, e.g., for the tested prototype and $N = 300$ turns $F_{elm} = 0.015\,N$ when $I = 0.01$ A and $F_{elm} = 0.107$ N when $I = 0.07$ A.

Although theoretically justified, equations derived in [12], not always give the expected results.

If a load impedance $\mathbf{Z_L} = R_L + jX_L$ is connected across the coil terminals, a closed electrical circuit will be created. The *rms* current I in the circuit and *rms* voltage V across the load impedance $\mathbf{Z_L}$ are, respectively,

$$I = \frac{E}{\sqrt{(R_c + R_L)^2 + (X_c + X_L)^2}} \approx \frac{E}{R_c + R_L} \tag{13}$$

$$V = I\sqrt{(R_L^2 + X_L^2)} \tag{14}$$

where $\mathbf{Z_c} = R_c + jX_c$ is the internal impedance of the coil. Since the coil is not furnished with any ferromagnetic core and the vibration frequency is low (usually less than 30 Hz), Hz), $R_c \gg X_c$. For resistive load the load inductance X_L can also be neglected. The output active power of the device can simply be found as:

$$P_{out} = I^2 R_L \tag{15}$$

where R_L is the load resistance. Further, the current I can be rectified and used for charging a battery, which in turn energizes an electronic device, e.g., a wireless sensing system [7,12].

The maximum output power is at resonance, i.e. $\omega = \omega_{nat}$. Combining together eqns (2), (9), (10), (13) and (15), assuming $R_c \gg X_c$, and neglecting the load inductance X_L, the maximum output power is

$$P_{max} \approx \frac{\alpha_i^2}{2\varsigma^2}\left(\frac{NB_m l_M F_m}{\omega_{nat} M}\right)^2 \frac{1}{R_c^2 / R_L + 2R_c + R_L} \tag{16a}$$

For $R_L = R_c$ eqn (16a) takes simpler form, i.e.,

$$P_{max} \approx \frac{\alpha_i^2}{\varsigma^2}\left(\frac{NB_m l_M F_m}{\omega_{nat} M}\right)^2 \frac{1}{8R_c} \tag{16b}$$

The output power of an electromechanical device with cantilever beam is high when:

- the damping ς, natural frequency ω_{nat}, tip mass M, and coil resistance R_c are low;
- the number of turns N, magnetic flux density B, length of magnets l_M, and amplitude of external force F_m are as high as possible.

High magnetic flux density B in the air gap can be maintained if high energy PMs are used and the gap between PM poles is small. Fig. 4 shows the maximum power at resonance (f_{nat} = 17.1 Hz) generated by the investigated energy harvesting device as a function of the damping ζ coefficient. Even for very low damping coefficient $\varsigma =$ = 0.05 the maximum output power does not exceed 65 mW.
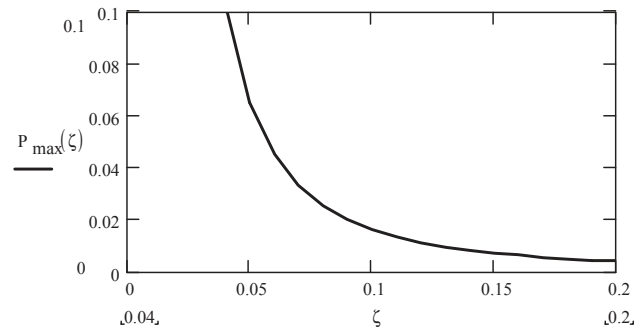
Fig 4. Maximum output power (W) generated by the investigated energy harvesting device at resonant versus damping ζ coefficient ζ for f_{nat} = 17.1 Hz, N = 200, B = 0.85 T, l_M = 11 mm, $F_m = M{\cdot}g$ = 0.819 N, M = 0.083 kg, R_c = 6.93 Ω, and R_L = 4.7 Ω.

4. PROTOTYPE

On the basis of eqns (1) to (16) a prototype of a small energy harvesting electromechanical device (Fig. 5) has been designed and built for research purposes. Specifications are given in Table I. As a cantilever beam (flat spring) both steel and beryllium copper ribbons have been used. The natural frequency of the spring – mass system can be adjusted either by changing the length L of the cantilever beam or adding more than one spring in parallel. The stationary coil has been wound with round copper wire. The coil has three taps (100+100+100) and the total number of turns N = 300.
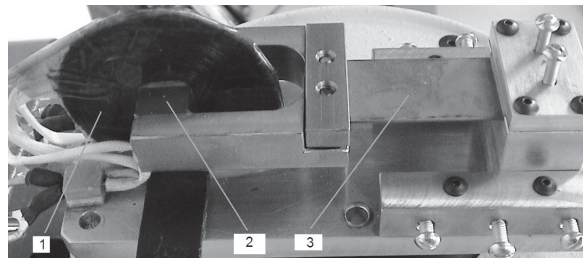

Fig. 5. Prototype of the energy harvesting electromechanical device: 1 – coil, 2 – PM, 3 – cantilever beam.

Table 1. Specifications of energy harvesting electromechanical device.

|	
Dimensions of a single PM	$l_M = w_M = 11$ mm, $h_M = 8$ mm
Material of PMs	Sintered NdFeB, $B_r = 1.3$ T
Number of poles	2
Number of turns (tapped winding)	100 + 100 + 100 (max. 300)
Wire diameter	0.255 mm (AWG 30)
Air gap between PMs	4 mm
Mass of vibrating system with PMs (tip mass)	0.083 kg
Mass of cantilever beam per length	0.015 kg/m
Thickness of cantilever beam	0.10 mm
Width of cantilever beam	19.15 mm
Length of cantilever beam	Adjustable from 5 to 45 mm
Natural frequency	Adjustable from 8 to 30 Hz
Material of flat spring	Steel (alternatively beryllium copper)
Coil thickness	2 mm
Coil resistance (200 turns)	6.93 Ω
Coil resistance (300 turns)	10.27 Ω
Coil inductance (200 turns)	13.2 μH
Coil inductance (300 turns)	29.8 μH
Damping factor ζ	Approximately 0.1
Measured maximum output power	10 to 18 mW
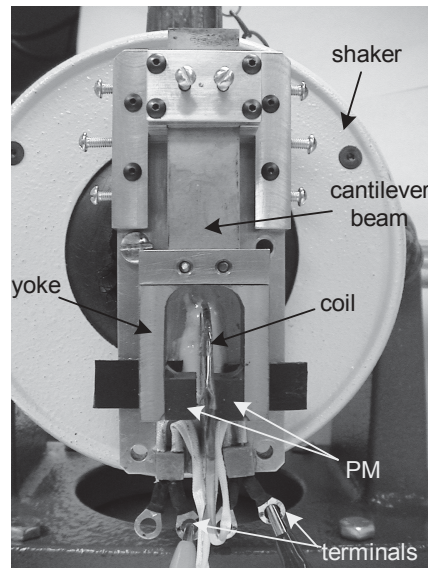
Fig. 6. Prototype of the energy harvesting electromechanical device placed on a small variable-frequency shaker

The device has been tested on a small shaker to provide a variable-frequency, variable-amplitude vibration. The electrical quantities have been measured using a multi channel oscilloscope. The acceleration of the shaker has been measured using a piezoelectric accelerometer. The energy harvesting device placed on the shaker is shown in Fig. 6.

5. MAGNETIC CIRCUIT

The magnetic circuit consists of two rectangular sintered NdFeB PMs and mild steel U – shaped yoke. The dimensions of PMs are as follows: axial length (along cantilever beam) l_M = 11 mm, width (perpendicular to the base) w_M = 11 mm, and height (parallel to the main magnetic flux) h_M = 8 mm.
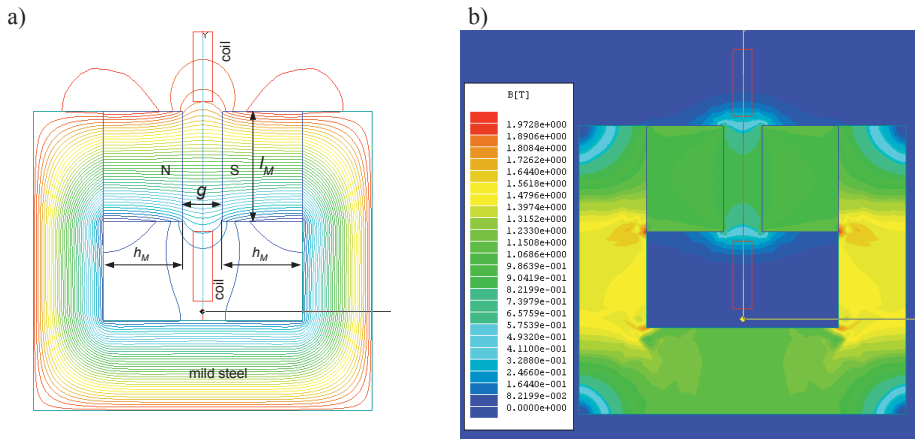
a)

b)

Fig. 7. Resultant magnetic field distribution excited by PMs and coil current (300 turns, 0.07 A): (a) magnetic flux lines; (b) magnetic flux density distribution. 2D FEM simulation.

The resultant 2D magnetic field distribution excited both by PMs and coil current as obtained from the FEM is shown in Fig. 7. The distribution of magnetic flux density excited by the coil alone (N = 300, I = 0.07 A) is shown in Fig. 8. The distribution of normal and tangential components of the magnetic flux density in the center line of the air gap excited by PMs is shown in Fig. 9. The distribution of normal and tangential components of the magnetic flux density along the center line of the air gap excited by the coil current (300 turns, 0.07 A) is shown in Fig. 10. Figs. 7 to 10 have been obtained using commercial 2D *Maxwell Ansoft* FEM software.
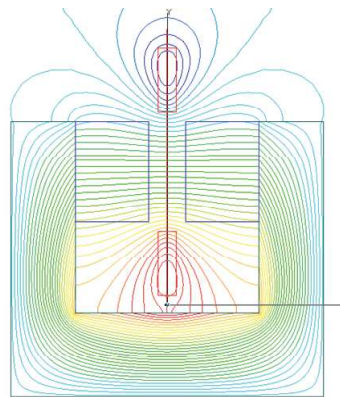

Fig. 8. Magnetic flux distribution excited by the coil with 300 turns and 0.07 A current. 2D FEM simulation.
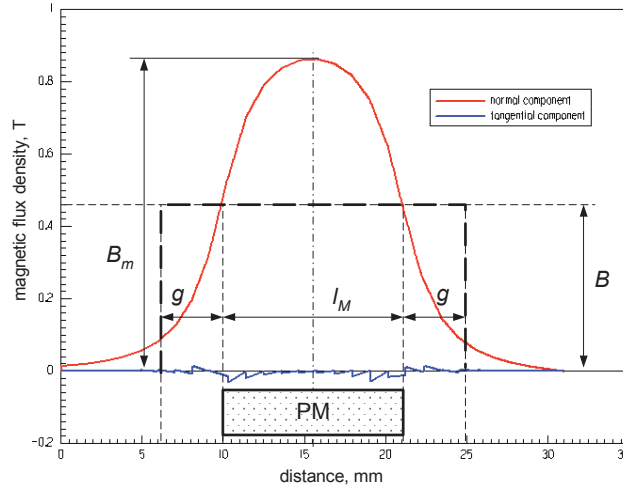
Fig. 9. Normal and tangential component distributions of the magnetic flux density excited by NdFeB PMs at zero coil current along the center line of the air gap (Tesla vs mm). 2D FEM simulation.
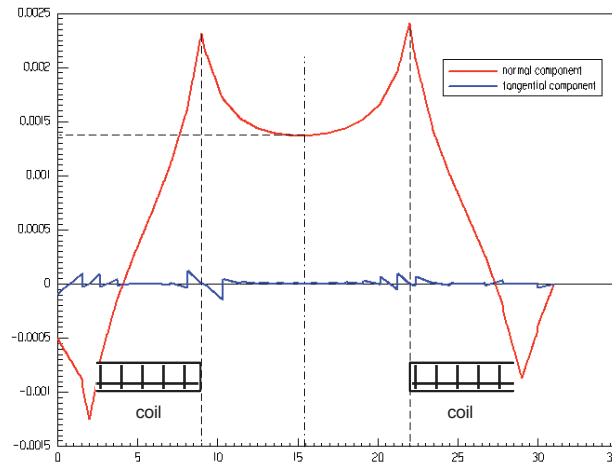

Fig. 10. Normal and tangential component distributions of the magnetic flux density excited by the coil current 0.07 A (300 turns) along the center line of the air gap (Tesla vs mm) assuming that PMs are removed. 2D FEM simulation.

Even for very high coil current (normally, a current lower than 0.07 A is induced), the normal component of the magnetic flux density excited by the coil MMF is negligible as compared with the magnetic flux density excited by PMs. For the center of the coil – magnet system, the normal component of the magnetic flux density excited by the coil is only 0.015 T while the magnetic flux density excited by PMs is 0.86 T. Thus the reaction of the coil currents can be neglected in calculation of the PM vibration generator. Also, the electromagnetic reaction force produced by the PM excitation field and coil current is small – eqn (12).

Similar value of the air gap magnetic flux density can be obtained analytically, i.e.:

$$B_m \approx \frac{B_r}{1 + \mu_{rrec} g / h_M} ,\tag{17}$$

where B_r is the remanent magnetic flux density, μ_{rrec} is the relative recoil magnetic permeability, g is the air gap (magnet-to-magnet), and h_M is the PM height per pole. For the tested prototype $B_r = 1.3$ T, $\mu_{rrec} = 1.089$, $g = 4$ mm, and $h_M = 8$ mm that gives $B_m = 0.842$ T. From Kirchhoff's equation for the magnetic voltage

$$2\frac{B_r}{\mu_o \mu_{rrec}} h_M = 2\frac{B_m}{\mu_o}\left(\frac{h_M}{\mu_{rrec}} + gk_{sat}\right),\tag{18}$$

where the saturation factor of the magnetic circuit

$$k_{sat} = 1 + \frac{\sum_i H_{Fei} l_{Fei}}{2B_m g / \mu_o} \geq 1 .\tag{19}$$

In the above eqn (19) $\Sigma H_{Fei} l_{Fei}$ is the magnetic voltage drop in the mild steel portions of the magnetic circuit, H_{Fei} is the magnetic field intensity in the ith portion of the magnetic circuit, and l_{Fei} is the length of the ith portion of the magnetic circuit. The saturation factor of the tested prototype is very close to unity (unsaturated magnetic circuit) because the air gap is large ($g = 4$ mm).

6. COMPARISON OF CALCULATIONS WITH TEST RESULST

Fig. 11 shows a comparison of the output (terminal) voltage and Fig. 12 shows the comparison of the *rms* current and output power obtained from calculations and measurements. The natural frequency of the cantilever beam has been adjusted to $f_{nat} = 17.1$ Hz ($L = 10$ mm). The load impedance connected across 200 turns (second tap) is $Z_L = (4.7 + j2\pi \, f 10.0 \times 10^{-6})\,\Omega$. The discrepancy between calculation and measurements is mainly due to low accuracy of analytical prediction of the spring constant k given by eqn (1) and measurement of damping coefficient ζ.
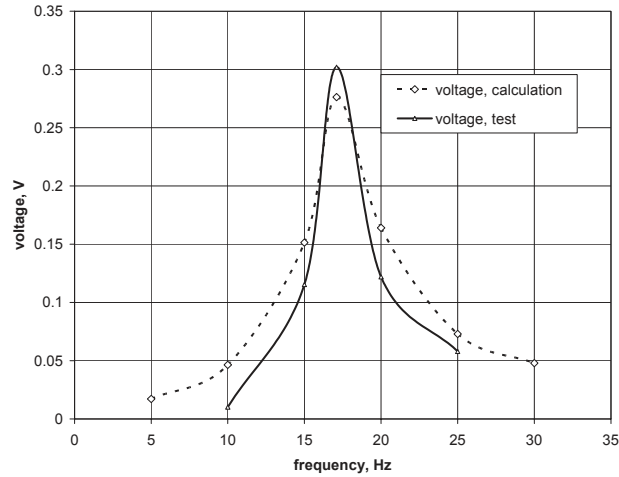
Fig 11. Comparison of the output voltage as a function of frequency obtained from calculations and measurements at natural frequency f_{nat} = 17.1 Hz (L = 10 mm), load impedance $Z_L = (4.7 + j2\pi\, f 10.0 \times 10^{-6})\Omega$, and 200-turn coil impedance $Z_c = (6.93 + j2\pi\, f 13.2 \times 10^{-6})\Omega$.
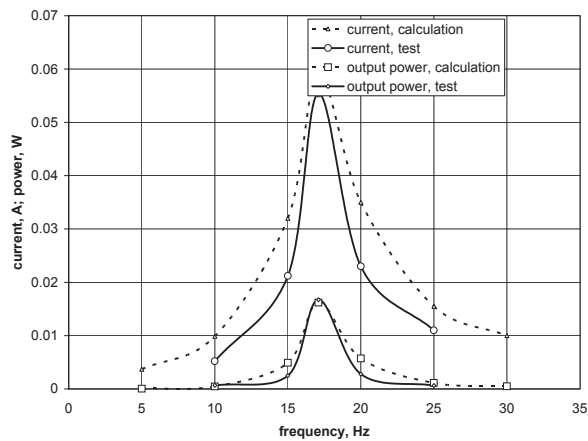

Fig 12. Comparison of the output *rms* current and output true power as a function of frequency obtained from calculations and measurements at natural frequency f_{nat} = 17.1 Hz (L = 10 mm), load impedance $Z_L = (4.7 + j2\pi\, f 10.0 \times 10^{-6})\,\Omega$, and 200-turn coil impedance $Z_c = (6.93 + j2\pi\, f 13.2 \times 10^{-6})\,\Omega$.
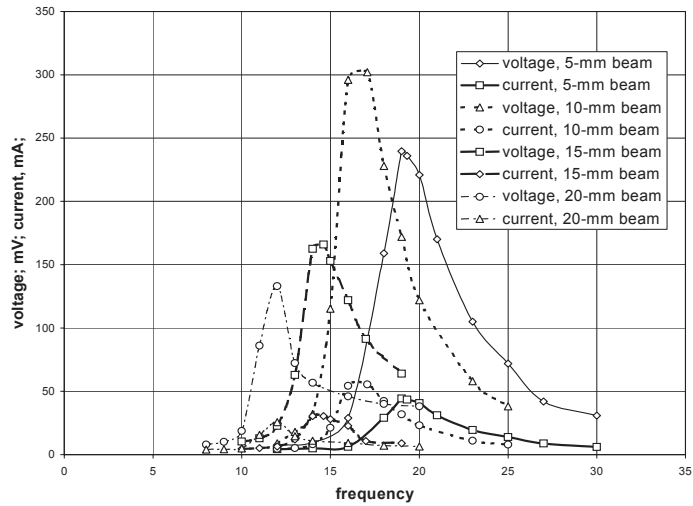
Fig. 13. Voltage and current versus frequency for different lengths of the steel spring (cantilever beam). Test results for load impedance $Z_L = (4.7 + j2\pi\,f10.0\times10^{-6})\,\Omega$.
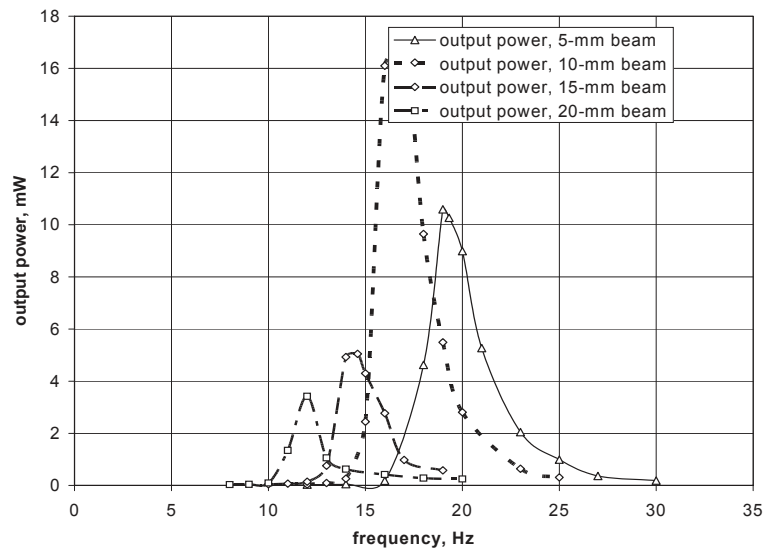

Fig. 14. Output power versus frequency for different lengths of the steel spring. Test results for load impedance $Z_L = (4.7 + j2\pi\,f10.0\times10^{-6})\,\Omega$.
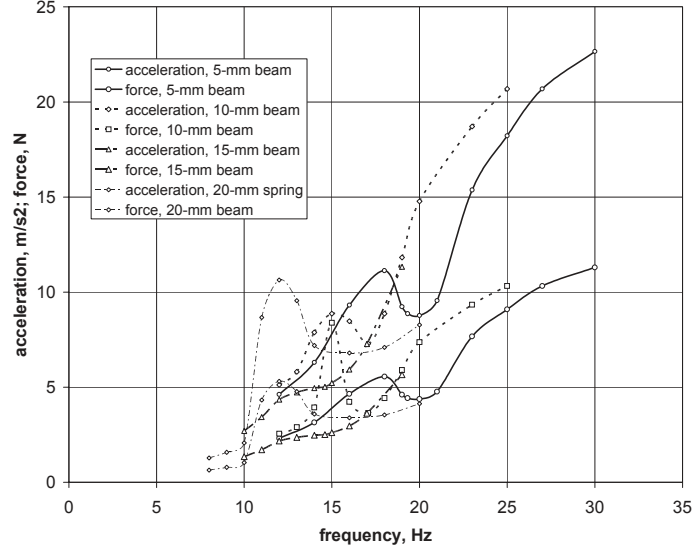
Fig. 15.   Acceleration and accelerating force versus frequency for different lengths of the steel
spring. Test results for load impedance $Z_L = (4.7 + j2\pi\ f 10.0 \times 10^{-6})\ \Omega$.

Test results for different lengths of steel springs (cantilever beams) are shown in
Figs 13, 14. and 15. The *rms* voltage and *rms* current versus frequency are plotted in
Fig. 13. The maximum voltage and maximum current depend on the length of the
spring. For the tested prototype the spring with the length of 10 mm (natural frequency
f_n = 17.1 Hz) at the load impedance $Z_L = (4.7 + j2\pi\ f 10.0 \times 10^{-6})\ \Omega$ provides the maxi-
mum voltage and maximum current. Consequently, for these parameters, the output
power also takes its maximum value (Fig. 14). The power factor is high, very close to
unity, because the load reactance is negligible. The linear acceleration and accelerating
force (Fig. 15) are also very sensitive to the spring length.

7. SELF ADJUSTABLE DEVICE

In practice, the frequency *f* of vibration can change in wide range, usually from
a few up to hundreds Hz, depending on the application. To maximize the efficiency of
the energy harvesting electromechanical device, the natural frequency f_{nat} should be
automatically adjusted to the frequency of vibration *f*. According to eqn (2) and Fig. 2,
the simplest method is to control the length *L* of the cantilever beam (flat spring). This
can be done by an electromechanical linear actuator and position control. If the fre-
quency of vibration *f* increases, the length of the cantilever beam *L* should be reduced
and extended if the frequency of vibration *f* decreases. There is no need for an additional
sensor or encoder since the output frequency of the energy harvesting device can be
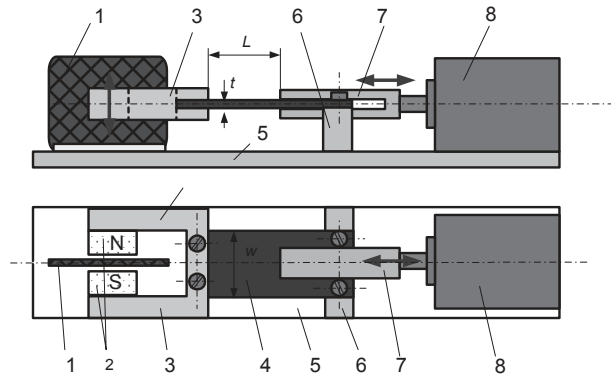used as a feedback signal.

Fig. 16. Electromechanical energy harvesting device with adjustable cantilever beam: 1 – stationary coil, 2 – PMs, 3 – mild steel yoke (return path for magnetic flux), 4 – cantilever beam (flat spring), 5 – base, 6 – spring holder and guidance, 7 – U-shaped stabilizer, 8 – actuator [13].

Fig. 16 shows the energy harvesting electromechanical device with self-adjustable natural frequency of the spring-mass system [13]. The coil 1, PMs 2, magnetic circuit 3, cantilever beam 4, and base 5 are the same as in the case of constant natural frequency energy harvesting device presented in Fig. 1. One end of the adjustable cantilever beam 4 is permanently fixed to the support 6 which serves also as the guidance for the cantilever beam 4 and stabilizer 7. The U – shaped stabilizer 7 is driven by a linear actuator 8. The natural frequency of the cantilever beam is controlled by inserting the beam more or less into the slot of the stabilizer 7. The stiffness (thickness) of the stabilizer must be much higher than that of the cantilever beam, otherwise the adjustment of the natural frequency would be weak. The cantilever beam 4 is stationary while only the stabilizer is pushed towards the beam or pulled out in the opposite direction.

Even a powerful PM brushless or stepping linear motor may develop lower electromagnetic force density than a roller screw or ball lead screw actuator. This is why a linear actuator with rotary motor and roller screw or ball lead screw can provide better packaging than a direct drive linear PM brushless motor.

A linear PM motor consumes much more electrical energy than a linear actuator with rotary motor and roller or ball lead screw of similar rating. Although, direct drive linear motors provide more accurate positioning at higher speeds, these machines are characterized by much lower force density than linear actuators with rotary motors and roller or ball lead screws. In this case, a small size of the actuator and very low power consumption are extremely important.

The implementation of the control system for self-adjustment of the cantilever beam natural frequency is shown in Fig. 17. The transfer function of the energy harvesting device is expressed by eqn (25) in Appendix II. The frequency of the current in the coil is used as a feedback signal and then compared with the frequency of the source of vibration. The frequency error signal is amplified and the output current of the servo amplifier feeds the stator winding of the actuator.
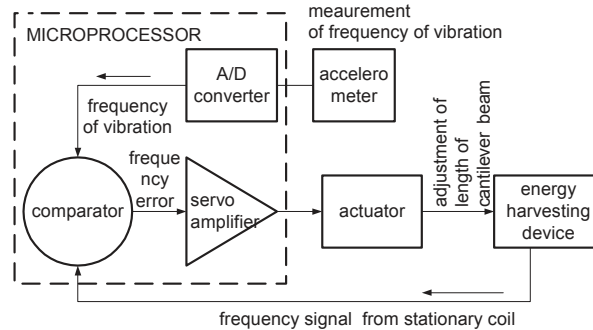
Fig. 17. Example of control circuit for adjustable cantilever length.

8. CONCLUSIONS

There is a physical limit imposed on the maximum output power of an electrome-
chanical energy harvesting device with cantilever beam expressed by eqn (16). The out-
put power is high when:
- the damping ς, natural frequency ω_{nat}, tip mass M, and coil resistance R_c are low,
- the number of turns N, magnetic flux density B, length of magnets l_M, and amplitude
  of external force F_m are as high as possible.

The investigated energy harvesting electromechanical devices shows the following
advantages:
- simple construction,
- provides low cost due to reduced number of parts, easy fabrication, and easy instal-
  lation,
- high efficiency of conversion of vibrational energy into electrical energy in the case
  of adjustable length of cantilever beam (flat spring) and its natural frequency to the
  frequency of external vibration,
- eliminates external electrical power and wiring,
- ideal for sensors installed in tracks, trailers, and containers where the frequency of
  vibration is variable,
- ideal for sensors installed on rotating parts,
- the device is environmentally friendly,
- slip rings and induction loops are eliminated,
- the device is maintenance free – no battery replacement,
- high reliability;
- ability to scale down to MEMs level (micro-collisions, air friction dissipation, and
  cushioning effects must be included).

On the other hands, the designer of energy harvesting electromechanical devices
must be aware of the following drawbacks and risks:
- Owing to application of electromechanical actuator and spring stabilizer, the volume
  of self-adjustable electromechanical energy harvesting device is bigger than that of
  an equivalent standard device that operates at constant natural frequency;

- Owing to application of high energy NdFeB PMs, there is a limit on ambient temperature. If ambient temperature exceeds 50 to 60^0C, the performance, especially the output power, deteriorates;
- PMs can accumulate ferromagnetic particles and debris in the air gap area between poles and coil;
- The spring, spring support, and U – shaped stabilizer may require lubrication.

APPENDIX I. MODELING OF VIBRATION OF CANTILEVER BEAMS BY ELEMENTARY BEAM THEORY

The static deflection of the cantilever beam as a function of the x coordinate is expressed as [4,5]:

$$x(y) = \frac{F_o}{6EI_a}(y^3 - 3Ly^2) \quad 0 \leq y \leq L, \tag{20}$$

where x is the deflection along the beam span y, F_o is the tip load, E is Young's modulus, I_a is the area moment of inertia, and L is the beam length. The tip deflection $\delta x(L)$ at $y = L$ and corresponding spring constant k are

$$\delta = x(L) = -\frac{1}{3}\frac{F_o L^3}{EI_a} = -\frac{F_o}{k} \quad k = \frac{3EI_a}{L^3}. \tag{21}$$

The dynamics of vibration for given mode shape or characteristic deflection shape can be described by the following spring-mass equation, in which $\delta(t)$ is a function of time t, i.e.:

$$m\ddot{\delta}(t) + k\delta(t) = F_o. \tag{22}$$

The above eqn (22) is an idealization of a cantilever beam [5]. Thus, the modal mass m is eqn (22) is not the same as the mass of the total cantilever beam $m_b = \rho w\, t\, L$. The modal mass can be obtained from the kinetic energy of the spring-mass system, i.e.:

$$E_k = \frac{1}{2}m\dot{\delta}^2(t) = \frac{1}{2}\left(\frac{33\rho wtL}{140}\right)\dot{\delta}^2 \tag{23}$$

The right hand side of eqn (23) has been found with the aid of eqns (20) and (21) [5]. The modal mass in eqn (22) is equal to (Fig. 22a):

$$m = \left(\frac{33\rho wtL}{140}\right) = \left(\frac{33m_b}{140}\right) = 0.2357m_b \tag{24}$$

Thus the vibration frequency for the modal shape $n = 1$ of the modal eqn (18) is found as [5]:

$$\omega_1 = \sqrt{\frac{k}{m}} = a_1\sqrt{\frac{EI_a}{\rho wtL^4}} \quad a_1 = 3.52 \tag{25}$$

Table 2 shows the first three vibration modes, modal mass, and coefficient a_n of a cantilever (clamped-free) beam. The values of coefficient a_n are according to [5].

Table 2. Transverse vibrations for cantilever beam.

vibration mode		modal mass	a_n
	a_1	0.2357 m_b	3.52
	a_2	0.0062 m_b	22.0
	a_3	0.00079 m_b	61.7

If a tip mass M is attached (Fig. 18b), the equation of motion (18) and spring constant (1) remain the same provided that the modal mass (20) is replaced by

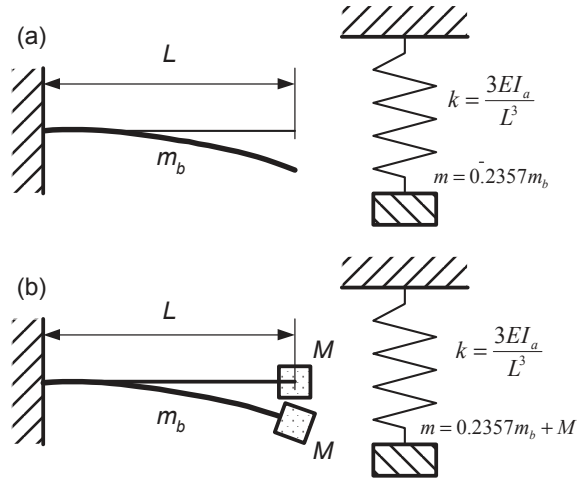$$m = 0.2357m_b + M \qquad (26)$$

Fig. 18.   Modeling cantilever beam by an equivalent spring-mass system: (a) without any tip mass; (b) with tip mass attached.

APPENDIX II. TRANSFER FUNCTION AND TIME RESPONSE

The Laplace transform of eqn (6) is

$$m[s^2 X(s) - sx(0) - \dot{x}(0)] + c[sX(s) - x(0)] + kX(s) = F(s) \ . \qquad (27)$$

Assuming that the initial displacement and velocity are zero, i.e., $x(0) = \dot{x}(0) = 0$, eqn (27) may be expressed as

$$G(s) = \frac{X(s)}{F(s)}; \quad G(s) = \frac{1}{ms^2 + cs + k}, \qquad (28)$$

where $G(s)$ is the transfer function (TF). The time-domain solution of the Laplace transform equation can be obtained by applying the inverse Laplace transform. For a unit impulse $X(s)=1$, the time response expressed in seconds is:

$$x(t) = 2me^{-\left(\frac{c}{2m}\right)t} \frac{\sin\left(\frac{\sqrt{4mk-c^2}}{2m}t\right)}{\sqrt{4mk-c^2}}, \tag{29}$$

Fig. 19. shows the theoretical time response (29) for the tested energy harvesting device
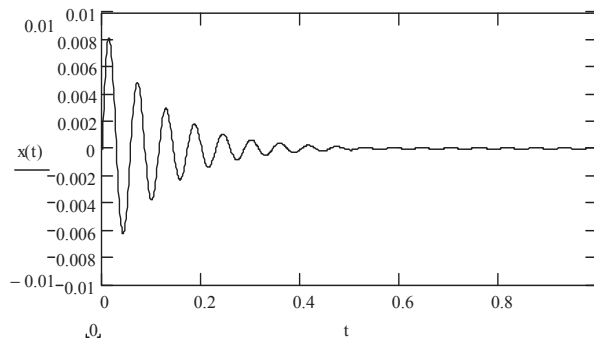

Fig. 19.   Theoretical time response (seconds) for $m = 0.083$ kg, $k = 1005.4$ N/m, $\omega_{nat} = 107.4$ rad/s ($f_{nat} = 17.1$ Hz), $c = 1.466$ kg/s, and $\zeta = 0.08$. Remaining data are given in Table 1.

BIBLIOGRAPHY

[1] Amirtharajah R., Chandrakasan A.P., 1998: *Self-Powered Signal Processing Using Vibration-Based Power Generation*, IEEE Journal of Solid State Circuits, Vol. 33, No. 5, 687-695.

[2] Ching N.N.H., Wong H.Y., Li W.J., Leong, P.H.W. Wen, Z., 2002: *A laser-micro machined multi-modal resonating power transducer for wireless sensing systems*, Sensors and Actuators, Elsevier, vol. A 97-98, 685-690.

[3] Choi H.Y., Jung S.Y., Jung H.K., 2002: *Performance Evaluation of Permanent Magnet Linear Generator for Charging the Battery of Mobile Apparatus,* Int. Conf. On Electr. Machines ICEM'2002, Brugges, Belgium, paper No 234 (CD).

[4] Craig R.R., 1981: *Structural Dynamics: An Introduction to Computer Methods*, J. Wiley & Sons.

[5] Den Hartog, J.P., 1984: *Mechanical Vibrations*, Dover Publications.

[6] Glynne-Jones P., Tudor M.J., Beeby S.P., White N.M., 2004: *An electromagnetic, vibration-powered generator for intelligent sensor systems,* Sensors and Actuators, Elsevier, vol. A110, 344-349.

[7] Lee J.M.H., Yuen S.C.L., Luk M.H.M., Chan G.M.H., Lei K.F., Li W.J., Leong P.H.W, Yam Y., 2003: *Vibration-to-Electrical Power Conversion Using High-Aspect-Ratio MEMS Resonators,* Power MEMS Conf., Chiba, Japan.

[8] Meninger, S., Mur-Miranda, J.O., Amirtharajah, R., Chandrakasan, A.P., and Lang, H.J., 2001: *Vibration-to-Electric Energy Conversion,* IEEE Trans. on VLSI Systems, Vol. 9, No. 1, 64-76.

  [9] Shearwood C., Yates R.B., 1997: *Development of an Electromagnetic Microgenerator*,
       Electronics Letters, Vol. 33, No. 22, 1883-1884.
 [10] Shenck N.S., Paradiso J.A., 2001: *Energy Scavenging with Shoe-Mounted Piezoelectrics*,
       IEEE Micro, Vol. 21, No. 3, 30-42.
 [11] Sterken T., Baert K., Puers R., Borghs S.: *Power Extraction from Ambient Vibration,*
       Catholic University of Leuven, Leuven, Belgium.
 [12] Williams C.B., Yates R.B. 1995: *Analysis of a Micro-Electric Generator for Microsystems*,
       8th Intern. Conf. on Solid-State Sensors and Actuators and Eurosensors IX, Stockholm,
       Sweden, 369-372.
 [13] Gieras J.F., Oh J.H., Huzmezan M.: *Electromechanical energy harvesting system*, Int. Pat-
       ent Publ. WO 2007/044008 A1.

PRZENOŚNE URZĄDZENIE ELEKTROMAGNETYCZNE DO POZYSKIWANIA ENERGII: ANALIZA ORAZ BADANIA EKSPERYMENTALNE

Streszczenie

   Artykuł omawia projektowanie, analizę oraz parametry urządzenia prototypowego do pozy-
skiwania energii, pracującego na zasadzie elektromechanicznego przetwarzania energii. Energia
kinetyczna wejściowa w postaci energii wibracji mechanicznych jest przetwarzana na energię
elektryczną (na zaciskach wyjściowych). Układ *sprężyna – masa* z ruchomym magnesem trwa-
łym jest pobudzany mechanicznie przez wibracje zewnętrzne. Napięcie elektryczne jest induko-
wane w cewce stacjonarnej, na skutek wibracji biegunów magnesów trwałych. Kiedy cewka
zostanie obciążona przez impedancję zewnętrzną, w obwodzie zewnętrznym popłynie prąd elek-
tryczny proporcjonalny do wzniecanej SEM w cewce. Równania podstawowe do obliczania
parametrów i charakterystyk zostały wyprowadzone na podstawie teorii elementarnej belki pod-
partej, analizy obwodowej oraz analizy polowej. Obliczenia teoretyczne zostały zweryfikowane
pomiarami na zbudowanym prototypie.

Słowa kluczowe: pozyskiwanie energii, generator wibracyjny, elektromechaniczny, magnesy
                  trwałe